

# Robust Worst-Case Design for Optimizing Average Performance in OFDM using Quantized CSI

Ana B. Rodríguez-González, Luis M. Lopez-Ramos, Antonio G. Marques, Javier Ramos, and Antonio J. Caamaño

Dept. of Signal Theory and Communications, Rey Juan Carlos University, Camino del Molino s/n, Fuenlabrada, Madrid 28943, Spain.

{anabelen.rodriquez, luismiguel.lopez,antonio.garcia.marques,javier.ramos,antonio.caamano}@urjc.es

**Abstract**—Orthogonal frequency-division multiplexing (OFDM) has been able to successfully exploit channel state information (CSI) at the transmitter, allowing to implement dynamic resource allocation schemes that improve spectral efficiency and error resilience. Nevertheless, in most wireless communication systems achieving a perfect CSI at the transmitter is difficult. For this reason a limited-rate feedback mode has been proposed, in which only quantized CSI at the transmitter is available through a finite number of bits that are fed back by the receiver. In this paper we resource allocation schemes for OFDM systems, that use limited-rate feedback and do not assume any structure on the channel quantizer. The new schemes are obtained by solving an optimization problem that maximizes average ergodic rate subject to average power and bit error rate constraints. The latter is satisfied by implementing a worst-case robust approach that reduces the dimensionality of the problem. The main burden is associated to the computation of optimal Lagrange multipliers. Provably convergent ensemble schemes that rely on the channel distribution as well as stochastic stochastic schemes that catch the average behavior of the system on-the-fly are developed for such task. Different alternatives to reduce the amount of feedback and the extension to multiple user systems wrap-up this paper.

**Index Terms**—OFDM, QoS in mobile systems, stochastic optimization, limited-rate feedback, resource management.

## I. INTRODUCTION

It is well known that spectral efficiency and error resilience in wireless Orthogonal frequency-division multiplexing (OFDM) systems improve with the knowledge of channel state information (CSI) at the transmitter (CSIT). Consequently, numerous schemes that rely on perfect (P-) CSIT have been proposed in the literature to optimize the performance of OFDM systems, typically by maximizing capacity or minimizing bit error rate (BER) [1].

Unfortunately, wireless channel variations, estimation errors, and feedback delay render the acquisition of P-CSIT difficult [1], [5]. These considerations motivated the development of a *limited-rate feedback* (LRF) mode, where only *quantized* (Q-) CSIT is available through a (typically small) number of bits that are fed back from the receiver. Q-CSIT entails a finite number of quantization regions describing different clusters of channel realizations. Firstly, the receiver estimates the channel and feeds back the index of the region that the current channel realization belongs to (channel codeword). Then, based on this codeword, the transmitter adapts its transmission parameters (here power and rate) accordingly. LRF modes are welcome because a finite feedback link is

affordable in most wireless systems, and because the Q-CSIT is robust to channel uncertainties. Prompted by these LRF features, several authors have investigated the problem of efficient OFDM resource allocation based on Q-CSIT; see e.g., [11], [3], [4], [2], [16]. A recent survey about the design of LRF in wireless systems can be found in [5].

In general, these authors deal with the optimization of power, rate or BER performance *per OFDM symbol*. Without assuming any structure on the channel quantizer, in this paper we design power and rate allocation schemes that based on Q-CSIT, optimize the *average* transmit-rate subject to average power and BER constraints. Averaging in the optimization problem is relevant because it gives rise to schemes amenable to practical implementation. Developed schemes operate in two phases: (i) an off-line phase that is carried before communication starts and where several parameters are computed; and (ii) an online phase that takes place during communication and where the receiver feeds the transmitter with the Q-CSIT back. Since our formulation involves average variables, the computational burden takes place during the initialization (off-line) phase and requires a *negligible burden during the transmission (online) phase*, which is certainly welcome from an implementation perspective. In fact, most of the design decisions through the paper are aimed to keep the computational burden low. The minimization of the average transmit-power in a setup with multiple users under more restrictive conditions than those here has been recently investigated in [6].<sup>1</sup>

## II. PRELIMINARIES

We consider wireless OFDM transmissions over  $K$  subcarriers through frequency-selective fading channels with discrete-time baseband equivalent impulse response taps  $\{h_n\}_{n=0}^N$ . Initially, a serial stream of data bits is demultiplexed to form  $K$  parallel streams indexed by  $k$ . Defining  $\mathbf{p}$  and  $\mathbf{r}$  as non-negative  $K \times 1$  vectors, stream  $k$  is next multiplied by a constant to load instantaneous power  $[\mathbf{p}]_k$ , and properly coded and modulated to give rise to an instantaneous transmit rate  $[\mathbf{r}]_k$ .

Once the proper set of operations are performed at both transmitter and receiver sides, the multipath fading frequency-selective channel is converted into a set of  $K$  parallel flat-fading subchannels each with fading power gain  $g_k$ , without loss of generality the noise power is assumed to be one. Channel estimation at the receiver relies on periodically inserted training symbols. When the channel is estimated, the

<sup>1</sup>*Notation:* Lower case boldface letters are used to denote vectors;  $[\cdot]_k$  denotes the  $k$ th entry of a vector;  $\mathbf{x} \geq \mathbf{0}$  means all entries of  $\mathbf{x}$  are nonnegative;  $\mathbb{E}_{\mathbf{x}}[\cdot]$  stands for the expectation operator over  $\mathbf{x}$ ;  $\lfloor \cdot \rfloor$  ( $\lceil \cdot \rceil$ ) denotes the floor (ceiling) operation;  $x^*$  the optimal value of variable  $x$ ; and  $[x]^+$  stands for  $\max(0, x)$ .

receiver has available a noise-normalized channel gain vector  $\mathbf{g} := [g_1; \dots; g_K]^T$ . While each realization of the gain vector  $\mathbf{g}$  constitutes the P-CSI, in Q-CSI approaches  $L$  quantization regions  $\mathcal{R}_l$  are selected, with  $l \in \{1, L\}$ . Different criteria have been proposed in the literature for efficiently defining these regions, some of which will be later summarized. Once the criterion is fixed, both transmitter and receiver know  $\mathcal{R}_l$ , and hence, only an index identifying the active region needs to be fed back from the receiver to the transmitter. Defining  $B := \lceil \log_2(L) \rceil$ , we denote by  $\mathbf{c} = \mathbf{c}(\mathbf{g})$  the  $B \times 1$  vector of bits used as the index of the region the current channel realization falls into. Clearly,  $\mathbf{c}$  is the piece of information that must be fed back to the receiver to the transmitter.

The ultimate goal of this paper is to find the appropriate allocation (loading) vectors  $\mathbf{p}$  and  $\mathbf{r}$  as a function of  $\mathbf{c}$ ; i.e.  $\mathbf{p}(\mathbf{c})$  and  $\mathbf{r}(\mathbf{c})$ . Since we have  $L$  different quantization regions, the latter will amount to design  $L$  non-negative  $K \times 1$  rate and power vectors denoted, respectively, by  $\mathbf{r}_l$  and  $\mathbf{p}_l$ . It is important to emphasize that so far no structure, neither for the channel quantizer nor for the rate-power codebook, has been assumed. With an eye on practicality, we will later discuss low complexity quantizers which presume an underlying structure.

To proceed with the design, the following assumptions are considered: (as1) *regions remain invariant over at least two consecutive OFDM symbols*; (as2) *the LRF channel is error-free and incurs negligible delay*; and (as3) *the instantaneous BER function per subcarrier denoted by  $\epsilon([\mathbf{p}]_k, [\mathbf{r}]_k, [\mathbf{g}]_k)$  is jointly convex with respect to  $[\mathbf{p}]_k$  and  $[\mathbf{r}]_k$ .*

Assumption (as1) allows each subchannel to vary from one OFDM symbol to the next so long as the quantization region in which it falls remains invariant; error-free feedback in (as2) is guaranteed with sufficiently strong error control codes, especially since data rates in the feedback link are typically low; and assumption (as3) will help the development of efficient algorithms and holds for many practical situations. An example of BER function satisfying (as3) is

$$\epsilon([\mathbf{p}]_k, [\mathbf{r}]_k, [\mathbf{g}]_k) = \kappa_1 \exp\left(-\kappa_2 [\mathbf{p}]_k [\mathbf{g}]_k / (2^{[\mathbf{r}]_k} - 1)\right), \quad (1)$$

for  $[\mathbf{g}]_k > (2^{[\mathbf{r}]_k} - 1)/[\mathbf{p}]_k$ . The value of constants  $\kappa_1$  and  $\kappa_2$  depend on the specific modulation and code implemented. The accuracy of (1) for (un)coded QAM modulations is widely accepted; see, e.g., [1].

### III. OPTIMAL DESIGN

#### A. Problem Formulation

The first step to formulate the optimization problem is to find the expressions for the average transmit-rate  $\bar{r}$  and transmit-power  $\bar{p}$  over all subcarriers. Since  $\mathbf{p}_l$  and  $\mathbf{r}_l$  are<sup>2</sup> the instantaneous power and rate values that the system will load when  $\mathbf{g} \in \mathcal{R}_l$ , the expressions for  $\bar{r}$  and  $\bar{p}$  are  $\bar{r} := \sum_{k=1}^K \mathbb{E}_{\mathbf{g}}[[\mathbf{r}_l(\mathbf{g})]_k] = \sum_{k=1}^K \sum_{l=1}^L [\mathbf{r}_l]_k \Pr\{\mathbf{g} \in \mathcal{R}_l\}$  and  $\bar{p} := \sum_{k=1}^K \mathbb{E}_{\mathbf{g}}[[\mathbf{p}_l(\mathbf{g})]_k] = \sum_{k=1}^K \sum_{l=1}^L [\mathbf{p}_l]_k \Pr\{\mathbf{g} \in \mathcal{R}_l\}$ , respectively.

Our goal is to maximize  $\bar{r}$ , subject to an average power constraint. Specifically, we want to constrain the *average* power across all subcarriers, i.e.,  $\bar{p} \leq \bar{p}_0$ . Additionally, to

put into practice power spectral masks we constrain the *instantaneous* power transmitted on subcarrier  $k$ ,  $[\mathbf{p}_l]_k \leq p_k^{\max}$ . Note that the constraint is different for each  $k$  because spectral masks depend on the frequency of operation. Moreover, we also want to impose a maximum BER  $\bar{\epsilon}_0$  for our system. To do so one could impose the average BER to satisfy  $\mathbb{E}_{\mathbf{g} \in \mathcal{R}_l}[\epsilon([\mathbf{p}_l]_k, [\mathbf{r}_l]_k, [\mathbf{g}]_k)] \leq \bar{\epsilon}_0 \forall k, l$ . However, this would increase the complexity of the algorithms to be developed. Instead, we advocate for a robust design where the maximum BER within a region (i.e., the BER corresponding to the worst channel realization) is bounded by  $\bar{\epsilon}_0$ . To this end, let  $[\mathbf{g}_l^{\min}]_k := \min\{[\mathbf{g}]_k \mid \mathbf{g} \in \mathcal{R}_l\}$  represent the worst channel gain in subcarrier  $k$  when  $\mathcal{R}_l$  is active. Then, we need  $\epsilon([\mathbf{p}_l]_k, [\mathbf{r}_l]_k, [\mathbf{g}_l^{\min}]_k) \leq \bar{\epsilon}_0$ . Since we want the transmit rate to be as high as possible, it is obvious that the previous constraint will be met with equality.

Analytically, the constrained optimization problem we aim to solve when solving (1) w.r.t. the rate loading, and is:

$$\begin{cases} \max_{\{\mathbf{p}_l\}, \{\mathbf{r}_l\}} \bar{r}, & \text{where } \bar{r} := \sum_{k=1}^K \mathbb{E}_{\mathbf{g}}[[\mathbf{r}_l(\mathbf{g})]_k] \\ \text{subject to:} & C1. \sum_{k=1}^K \mathbb{E}_{\mathbf{g}}[[\mathbf{p}_l(\mathbf{g})]_k] \leq \bar{p}_0, \\ & C2. \epsilon([\mathbf{p}_l]_k, [\mathbf{r}_l]_k, [\mathbf{g}_l^{\min}]_k) = \bar{\epsilon}_0, \quad \forall k, l, \\ & C3. 0 \leq [\mathbf{p}_l]_k \leq p_k^{\max}, \quad \forall k, l \\ & C4. [\mathbf{r}_l]_k \geq 0, \quad \forall k, l. \end{cases} \quad (2)$$

The objective in (2) is to maximize the average rate over all possible channel realizations. However, the constraints involve different forms of CSI:  $C1$  is an average requirement, while  $C2$ – $C4$  need to be satisfied per region  $l$  and subcarrier  $k$ . Even though constraint  $C1$  ensures that the average power does not exceed  $\bar{p}_0$ , it does not impose any limit on the instantaneous power transmitted during an OFDM symbol,  $\sum_{k=1}^K [\mathbf{p}_l(\mathbf{g})]_k$ , which is allowed to vary in time. As for the instantaneous upper bound in  $C3$ , it imposes power spectral mask constraints in every region.

**Remark 1:** Optimization throughout this paper is carried out for continuous-rate (CR) loadings. If needed, algorithms that transform the CR solution into a DR loadings are available in the literature; see, e.g., [9].

#### B. Finding the optimal solution

The problem in (2) is convex, thus it can be efficiently solved using a dual approach. First, let  $\beta_p$  denote the Lagrange multiplier associated with  $C1$ . Moreover, since  $C2$  establishes a one-to-one mapping between the rate and the power within a region, the BER can be inverted with respect to the rate. Let  $[\mathbf{r}_l]_k = \epsilon_r^{-1}([\mathbf{p}_l]_k, [\mathbf{g}_l^{\min}]_k, \bar{\epsilon}_0)$  denote such inverse function. Based on this notation, we can write the sufficient conditions for optimality of (2) as [cf. [10, pp. 316]]:

$$\frac{\partial \epsilon_r^{-1}([\mathbf{p}_l^*]_k, [\mathbf{g}_l^{\min}]_k, \bar{\epsilon}_0)}{\partial [\mathbf{p}_l]_k} - \beta_p^* = 0, \quad \forall (k, l) \quad (3)$$

and  $\sum_{k=1}^K \mathbb{E}_{\mathbf{g}}[[\mathbf{p}_l^*(\mathbf{g})]_k] = \bar{p}_0$ . If the multiplier  $\beta_p$  is known, the optimal powers in (3) can be easily found using a one-dimensional search. Note that if after solving (3) the optimum powers do not satisfy  $C3$ , the optimum *feasible* powers can be found by projecting each of the solutions of (3) onto the interval  $[0, p_k^{\max}]$ . To obtain the final rate loadings, the powers given by (3) need to be substituted into  $\epsilon_r^{-1}$ .

<sup>2</sup>The subscript  $l$  here will be also written explicitly as  $l(\mathbf{g})$  in places that this dependence must be emphasized.

The literature provides different methods that numerically search for the optimal values of the Lagrange multipliers. A successful one is the *method of the multipliers* [10, Eq. (4.35)]. If  $i$  stands for iteration index, and  $\mu(i)$  represents a non-increasing step-size, then the Lagrange multipliers are updated in the form

$$\beta^p(i+1) = \left[ \beta^p(i) + \mu(i) \left( \sum_{k=1}^K \mathbb{E}_{\mathbf{g}} [\mathbf{p}_{l(\mathbf{g})}(\beta^p(i))]_k - \bar{p}_0 \right) \right]^+ \quad (4)$$

It can be shown that for a broad range of stepsizes the iteration in (4) converges to a point for which the constraints are satisfied with equality (which is the overall global optimum if the original problem is strictly convex). Noticeably, convergence is attained also for sufficiently small *constant*  $\mu$ .

To clarify the design we next outline an algorithm to find the solution of (2).

---

**Algorithm 1: Robust Resource Allocation**

---

- (S1.0) Let  $i$  be an iteration number and set  $i = 0$ . Let  $\delta > 0$  be a small number. Start with arbitrary non-negative  $\beta^p(i)$ .  
(S1.1) Substitute  $\beta^p(i)$  into (3) to find  $\mathbf{p}_l^* \forall l$ . Set  $\mathbf{p}_l(i) = \mathbf{p}_l^*$ .  
(S1.2) Use  $\mathbf{p}_l(i)$  to check constraint C1 in (2). If  $|C1| < \delta p_0$  then *stop* and go to (S1.3); otherwise update  $\beta^p(i)$  according to (4), increase  $i$  and go to (S1.1).  
(S1.3) Substitute  $\mathbf{p}_l(i)$  into  $\epsilon_r^{-1}$  to find the final rate loadings. *Return*  $\{\mathbf{p}_l(i)\}_{l=1}^L$  and  $\{\mathbf{r}_l(i)\}_{l=1}^L$  as the optimal solution.
- 

Algorithm 1, is run off-line during an initialization phase so that the optimal power and rate loadings for all the regions are known by the transmitter before the communication starts. During the transmission phase, every time the channel changes (i.e., every coherence interval), the receiver finds  $\mathbf{c} = \mathbf{c}(\mathbf{g})$ , and feeds back that codeword to the transmitter. Based on  $\mathbf{c}$ , the transmitter selects the corresponding  $\mathbf{p}_l$  and  $\mathbf{r}_l$  vectors that are loaded during the current coherence time. As pointed out in the introduction, different from, e.g. [11] or [2], the average formulation in (2) leads to an online phase with negligible computational complexity.

### C. Stochastic Computation of the Lagrange Multipliers

The main burden of Algorithm 1 is associated with the computation of  $\beta^{p*}$ . As mentioned just before, the Algorithm 1 is performed off-line and requires knowledge of the channel statistics [cf. (4)]. However, there are situations where this computation cannot be efficiently carried out or is not even feasible, for example: in limited-complexity systems that cannot afford the off-line burden (for systems with high  $K$ , the number of regions  $L$  can be very high), or when the channel statistics are unknown. In those situations, stochastic approximation algorithms arise as an alternative solution to estimate  $\beta^p$  [7]. Let  $t$  denote the current block index (whose duration will correspond to the channel coherence interval  $T_{ch}$ ) and  $\mathbf{g}[t]$  the fading state during block  $t$ . To develop a stochastic version of Algorithm 1, we will drop the expectations over  $\mathbf{g}$  in (4), so that the average is replaced with an instantaneous (stochastic) estimate. This way, we get

$$\hat{\beta}^p[t+1] = \left[ \hat{\beta}^p[t] + \mu[t] \left( \sum_{k=1}^K [\mathbf{p}_{l(\mathbf{g}[t])}(\hat{\beta}^p[t])]_k - \bar{p}_0 \right) \right]^+ \quad (5)$$

For sufficiently small  $\mu$ , it can be shown that the trajectories of the iterations in (4) and (5) are locked. More specifically,

with similar initial conditions in (4) and (5) and given  $T > 0$ , there exists  $b_T > 0$ ,  $\beta_T > 0$  so that

$$\max_{1 \leq t \leq T/\mu} \|\beta^p(t) - \hat{\beta}^p[t]\| \leq c_T(\mu) b_T \quad 0 \leq \mu \leq \mu_T, \quad (6)$$

where  $c_T(\mu) \rightarrow 0$  as  $\mu \rightarrow 0$ . The result in (6) holds with probability one and can be proved based on the averaging approach in [12, Chapter 7].

It must be emphasized that iterations in (5) can be implemented online without knowing the channel PDF. Even more, since iterations in (5) rely on actual (real-time) channel measurements, they can be readily used when interference from other cells is present (in most cases, the PFD of interference is not known). Moreover, the iterations in (5) eliminate the need of implementing Algorithm 1 during a training (off-line) phase. Now, the operation for every  $t$  is as follows. The receiver finds  $\mathbf{c}$ , and feeds this codeword back to the transmitter. The transmitter receives the codeword  $\mathbf{c}$ , finds the corresponding  $\mathbf{p}_l$  substituting  $\hat{\beta}^p[t]$  into (3), and then finds  $\mathbf{r}_l$  substituting  $\mathbf{p}_l$  into  $\epsilon_r^{-1}$ . After this, the transmitter updates  $\hat{\beta}^p[t+1]$  according to (5) and transmits using  $\mathbf{p}_l$  and  $\mathbf{r}_l$  as the optimal power and rate loadings during block  $t$ . Hence, the offline phase is eliminated by slightly increasing the complexity during the transmission (online) phase.

## IV. ON THE STRUCTURE OF THE FEEDBACK CODEWORD

So far no prior structure of the channel quantizer was assumed. Since the entries of  $\mathbf{g}$  are positive real numbers, a popular low-complexity alternative quantizer consists of performing separate scalar quantization of each of the entries of  $\mathbf{g}$  [2], [6]. Remarkably, numerical results have consistently corroborated that for medium-high feedback rates, this assumption does not entail a significant loss of performance. When a scalar quantizer is implemented, each subcarrier is divided into  $L_k$  regions which can be described by a the pair of thresholds  $\mathcal{R}_{k,l} = [\tau_{k,l-1}, \tau_{k,l})$  with  $\tau_{k,0} = 0$  and  $\tau_{k,L_k} = \infty$ . There are several available alternatives to design the a scalar channel quantizer, see, e.g., [2, Sec. V]. A simple one that has shown to be effective is the equally-probable region quantizer in [2, Sec. V-B.2.a]. This quantizer determines  $\tau_{k,l}$ 's so that the probability of  $[\mathbf{g}]_k$  falling in any of the regions is  $1/L_k$ .

From an operational perspective, the main drawback associated with per subcarrier scalar quantizers is that in most OFDM systems, the number of subcarriers  $K$  is high, and therefore a large number of bits  $B = \lceil K \log_2(L_k) \rceil$  needs to be fed back. A variety of methods that exploit correlation among subcarriers to reduce the amount of feedback have been proposed in the literature. Here we focus on two of them.

### A. Subcarrier Grouping Algorithms

An alternative set of algorithms have been proposed for exploiting the correlation of subcarriers (e.g., [13]). The rationale for these methods is to first divide the set of correlated OFDM subcarriers into groups of subcarriers. Groups are defined using criteria such as statistical independence and the number of groups is typically set to a multiple of the channel length  $N+1$ . In fact, [2, Proposition 1] establishes that the minimum number of groups to have a reliable estimation is  $2N+1$ . Once the groups are defined, a gain representing the entire group is quantized and sent to the transmitter, which sets the quantized

gain of all the subcarriers in that group to the same value. Nevertheless, these methods have been shown to be effective in practice and due to its easy implementation they are widely used.

### B. Subcarrier Ordering Algorithms

A simple and highly effective new idea to reduce the feedback for the equally spaced case has been recently proposed in [8]. Instead of feeding back the subcarrier gains of all comb-type pilots, the algorithm in [8] sorts the channel gain of comb-type pilots and only feeds back: i) the permutation index that identifies the current ordering and ii) the quantized version of maximum and minimum channel gains, denoted by  $[g]_{min}$  and  $[g]_{max}$ . The order information is efficiently transferred by an index from a predetermined codebook, which contains all the possible orders of subcarrier channel gains and was shared by the transmitter and the receiver. If the number of pilots is denoted by  $G$  (recall that according to Property 1,  $G$  should be greater than  $2N$ ), then the gains of the remaining  $G - 2$  pilots are estimated by interpolation. A simple linear interpolation for the  $k$ th interpolated gain is given by

$$[\hat{g}]_k = \frac{[g]_{max} - [g]_{min}}{G - 1}(k - 1) + [g]_{min}. \quad (7)$$

The gains for the remaining subcarriers are estimated using the procedure described for the equally spaced case. The amount of feedback in this case is  $\lceil 2 \log_2(L_k) + \log_2(G!) \rceil$  bits (maximum and minimum gains, plus indexing all the  $G$  possible orders). This option can entail a reduction of the feedback rate if the number of regions  $L_k$  is high or if the number of taps  $N$  is small. Therefore, it represents a simple and effective trade-off between accuracy and complexity, specially for systems with low  $G$ .

### V. EXTENSION TO MULTIUSER SYSTEMS

The schemes that we have presented assume single user scenarios. Nevertheless, most OFDM wireless systems consider multiuser communications. Single user and multiple user adaptive OFDM systems differ in subcarrier assignment to users. Two alternatives arise to deal with this issue: fixed subcarrier assignment and (channel-)adaptive subcarrier assignment. When the subcarrier assignment is fixed (i.e., it is the same regardless of the CSI), the problem can be decoupled among users and our algorithms can be readily used in a multiuser architecture. It is important to mention though, that if the fixed subcarrier allocation is designed to collect the maximum frequency diversity (which in principle is the best option when the assignment is fixed), then the subcarriers assigned to a given user have to be equally spaced and as far apart as possible. The scenario where subcarrier assignment is adapted as a function of the CSI is more challenging. If the criterion to decide which user is going to access is fixed beforehand (e.g., the subcarrier is assigned to the user with highest SNR), then the schemes developed in this paper can still be used as long as the criterion is taken into account when the iterations over the Lagrange multipliers are implemented. However, if the subcarrier allocation is designed to be optimal in the sense of (2), then the developed schemes require changes that are non-trivial. Specifically, the subcarrier assignment

needs to be incorporated into (2) as a new optimization variable. The updated problem is more difficult to solve and can even have combinatorial complexity; see e.g., [6], [11], [14], and references therein.

### VI. NUMERICAL EXAMPLES

To numerically test our rate-efficient designs, an adaptive OFDM system with  $K = 64$  subcarriers is considered. Modulation and coding schemes satisfying (1) are assumed, a maximum BER level of  $\bar{\epsilon}_0 = 10^{-3}$  is required, and an average power budget of  $\bar{p}_0 = 100$  is available. Channel taps are assumed complex Gaussian (so that taps amplitudes are Rayleigh and subcarrier power gains are exponential).

**Test Case 1 (Comparison of allocation schemes):** For different average SNR values, Fig. 1 compares the *total* average transmit rate for five different allocation schemes. The number of regions is  $L_k = 3$  (since the first region will always be an outage region this implies 2 active regions per subcarrier) and the power profile considered for the multi-path channel corresponds to the test channel *Vehicular A* recommended by the ITU; see [6, Sec. V] for more details. The two first schemes are the P-CSIT benchmark (water-filling over subcarriers and time, penalized with a SNR gap of  $\log(\kappa_1/\epsilon_0)/\kappa_2$  [1]) and the Q-CSIT scheme developed in this paper. The two next schemes satisfy the requirements of the Wimax Standard [15]. Both use the same power for all subcarriers and consider different Modulation and Codification Schemes (MCS). The difference is that the first scheme (*Wimax 1*) uses the same MCS for every subcarrier, while the second scheme (*Wimax 2*) can use a different MCS on each subcarrier. For each channel realization the MCS mode selected is the one that satisfies the BER constraint and gives rise to the highest instantaneous transmit-rate. The fifth method that has been implemented (*Shin06*) was presented in [16]. It considers a finite number of rate values and transmits with the same power in all active subcarriers. The main difference relative to the previous schemes is that the power corresponding to subcarriers that are not activated can be used to increase the power of the active subcarriers (this amounts to a very simple form of power adaptation). For each channel realization, the active rate modes and the number of active subcarriers are selected so that the instantaneous BER constraint is satisfied and instantaneous transmit-rate is maximized.

Two are the most relevant observations: (i) the rate loss of our algorithm w.r.t. the P-CSIT benchmark is less than 15% (the gap reduces as the number of regions increases and it less than 0.5% for  $L = 32$ ; and (ii) our algorithm performs better than the other Q-CSIT schemes. Specifically, Algorithm 2 performs better than (*Sin06*), the latter performs better than (*Wimax 2*), and the latter better than (*Wimax 1*). This was expected because Algorithm 2 implements both rate and power adaptation per subcarrier, (*Wimax 2*) implements rate adaptation per subcarrier but a grossly suboptimal power adaptation, and (*Wimax 1*) only implements rate adaptation. It is worth noting that the relative gain of our algorithm is reduced for higher SNR. This is not surprising because it is known that power adaptation does not give significant gains in the high SNR range.

Numerical results confirming our previous conclusions are shown in subplot (b) of Fig. 1 for a setup with  $K = 256$ ,  $L_k = 4$ ,  $\epsilon_0 = 10^{-4}$  and  $p_0 = 400$ .

**Test Case 2 (Feedback reduction):** The final test case analyzes the performance loss when the alternatives to reduce the feedback rate presented in Section V are implemented. The number of regions per subcarrier is  $L_k = 4$ , a channel with  $N + 1 = 4$  taps is simulated, and different average SNR values are considered. Subplot (c) in Fig. 1 compares the average transmit rate achieved by Algorithm 1 for four different feedback schemes: i) a full-feedback scheme that sends information of all the subcarriers (128 feedback bits); iv) the scheme in Section IV-A that groups the subcarriers into  $2N + 1$  sets and quantizes the average gain of each set (16 feedback bits); and v) the scheme in Section IV-B that combines the ordering of the  $2N + 1$  pilots and the quantization of the maximum and minimum gains (20 bits). Moreover we also test more sophisticated schemes that instead of grouping subcarriers, insert equally spaced pilots and use estimation and interpolation techniques to find the value in the non-pilot subcarriers [2, Eq. (23) and Alg. RC1]. The main conclusion from plot (b) is that all tested methods exhibit a similar average rate. However, channel estimation errors will also affect the BER performance and can induce violation of the BER requirement. For this reason, the subplot (d) depicts the BER for the four tested schemes. Although the differences are not extremely high, we observe how indeed errors in channel estimation can entail a violation of the BER constraint. In particular, the larger BER for iii) is because when the subcarrier gains are sorted, they do not exactly follow a linear profile as assumed in (7). This results in an overestimation of the gains, and hence made the system transmitting a higher rate with higher error. Moreover we do not observe a significant advantage between the technique in [2, Eq. (23) and Alg. RC1] and the simple grouping strategy in IV-A. In a nutshell, the numerical results show that the described techniques are able to considerably reduce the amount of feedback, but at the cost of increasing the BER. This behavior clearly supports the utilization of resource allocation schemes that have been derived under a robust worst-case approach.

## VII. CONCLUDING SUMMARY

For OFDM systems that adapt instantaneous power and rate loadings based on quantized CSIT obtained through a limited-feedback rate link, schemes that maximize the average transmitted rate under prescribed average power and BER constraints were devised. Using optimization theory, the optimal power and rate codebooks have been found using a worst-case robust approach. Different schemes to find the Lagrange multipliers were developed and two alternatives that exploit the correlation among subcarriers to reduce the amount of feedback bits required were compared. Numerical results validate the simplifying assumptions and show that the proposed schemes are attractive because they incur a small loss relative to the benchmark design based on P-CSIT which requires often unrealistic feedback information.<sup>3</sup>

<sup>3</sup>The authors wish to thank Prof. J.L. Rojo-Alvarez and Prof. J. Requena-Carrion for helpful collaboration in this topic.

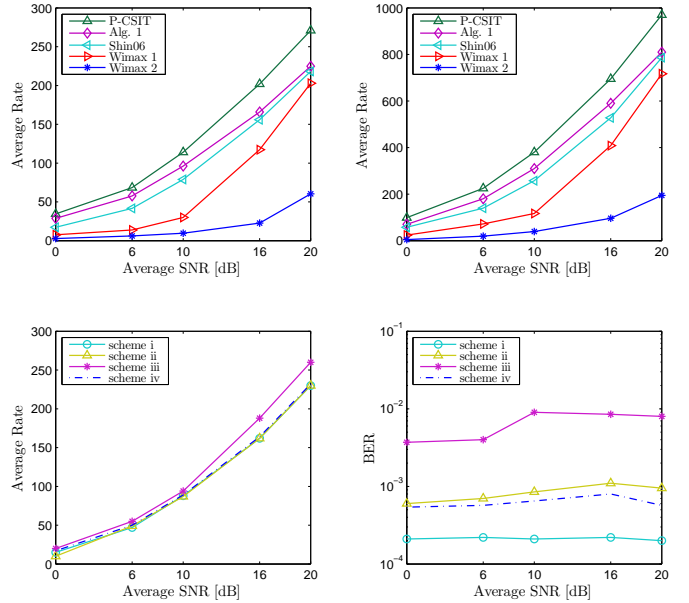


Fig. 1. Test case 1 (subplots a and b) and test case 2 (subplots c and d).

## REFERENCES

- [1] A. Goldsmith, *Wireless Communications*. Cambridge Univ. Press, 2005.
- [2] A. G. Marques, F. F. Digham, and G. B. Giannakis, "Optimizing power efficiency of OFDM using quantized channel state information," *IEEE J. Sel. Areas Commun.*, vol. 24, no. 8, pp. 1581–1592, Aug. 2006.
- [3] F. F. Digham and M. O. Hasna, "Performance of OFDM with M-QAM modulation and optimal loading over Rayleigh fading channels," in *Proc. of IEEE Veh. Tech. Conf.*, Los Angeles, CA, Sep. 2004, pp. 479–483.
- [4] P. Xia, S. Zhou, and G. B. Giannakis, "Adaptive MIMO OFDM based on partial channel state information," *IEEE Trans. Signal Process.*, vol. 52, no. 1, pp. 202–213, Jan. 2004.
- [5] D. J. Love, R. W. Heath, V. K. Lau, D. Gesbert, B. Rao, and M. Andrews, "An overview of limited feedback in wireless communication systems," *IEEE J. Sel. Areas Commun.*, vol. 26, no. 8, pp. 1341–1365, Aug. 2008.
- [6] A. G. Marques, G. B. Giannakis, F. Digham, and F. J. Ramos, "Power-efficient wireless OFDMA using limited-rate feedback," *IEEE Trans. Wireless Commun.*, vol. 7, no. 2, pp. 685–696, Feb. 2008.
- [7] X. Wang, G. B. Giannakis, and A. G. Marques, "A unified approach to QoS-guaranteed scheduling for channel-adaptive wireless networks," *Proc. IEEE*, vol. 95, no. 12, pp. 2410–2431, Dec. 95.
- [8] E. H. Choi, W. Choi, J. G. Andrews, and B. F. Womack, "Power loading using order mapping in OFDM systems with limited feedback," *IEEE Signal Process. Lett.*, vol. 15, pp. 545–548, 2008.
- [9] B. S. Krongold, K. Ramchandran, and D. L. Jones, "Computationally efficient optimal power allocation algorithms for multicarrier communication systems," *IEEE Trans. Commun.*, vol. 48, pp. 23–27, Jan. 2000.
- [10] D. P. Bertsekas, *Nonlinear Programming*. Athena Scientific, 1999.
- [11] C. Wong, R. Cheng, K. Lataief, and R. Murch, "Multiuser OFDM with adaptive subcarrier, bit, and power allocation," *IEEE J. Sel. Areas Commun.*, vol. 17, no. 10, pp. 1747–1758, Oct. 1999.
- [12] V. Solo and X. Kong, *Adaptive Signal Processing Algorithms: Stability and Performance*. Prentice Hall, 1995.
- [13] Z. Liu, Y. Xin, and G. B. Giannakis, "Space-time-frequency coded OFDM over frequency-selective fading channels," *IEEE Trans. Signal Process.*, vol. 50, no. 10, pp. 2465–2476, Oct. 2002.
- [14] R. Agarwal, V. Majjigi, Z. Han, R. Vannithamby, and J. Cioffi, "Low complexity resource allocation with opportunistic feedback over downlink OFDMA networks," *IEEE J. Sel. Areas Commun.*, vol. 26, no. 8, pp. 1462–1472, Oct. 2008.
- [15] *IEEE Std. 802.16-2009 Part 16: Air Interface for Broadband Wireless Access Systems*, 2009.
- [16] Y.-S. Shin, C. Mun, J.-G. Yook, Y.-J. Yoon, and H.-K. Park, "Capacity maximising efficient adaptive subcarrier selection in OFDM with limited feedback," *IEE Electron. Lett.*, vol. 42, no. 7, pp. 430–431, Mar. 2006.